



## CHAPTER II

### THEORETICAL BACKGROUND AND LITURATURE REVIEW

#### 2.1 Clay Minerals

Clay minerals, or phyllosilicate, consist of sheets of silica tetrahedral and alumina octahedral which are held together by only weak interatomic forces between the layers. Owing to their chemical composition and crystal structure, they are divided into four main groups which are illite, smectite, vermiculite and kaolite. Among these, the one that is found to be useful in the field of polymer composites is a group of expandable clay known as smectite clay.

Smectite clay is phyllosilicates or layer silicates having a layer lattice structure in which two-dimensional oxoanions are separated by hydrated cations (Kloprogge *et al.*, 1998). Montmorillonite, which is the main constituent of bentonites, is a mainly species of smectite clay. The structure of MMT is made of several stacked layers, with a layer thickness around 0.96 nm and a lateral dimension of 100-200 nm (Lertwimolnum and Vergnes, 2005). Its crystal lattice consists of a central octahedral sheet of alumina fused between two external silica tetrahedral sheets (in such a way that the oxygens from the octahedral sheet also belong to the silica tetrahedral), as shown in Figure 2.1. These layers organize themselves in a parallel fashion to form stacks with a regular gap between them, called interlayer or gallery (Manias *et al.*, 2001).

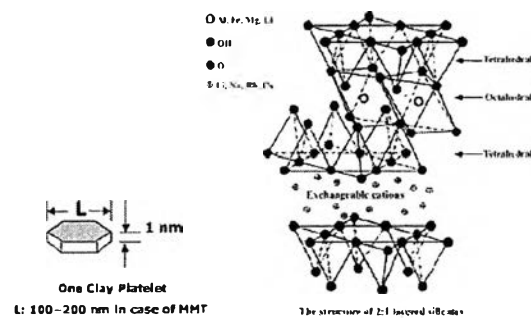


**Figure 2.1** Structure of montmorillonite ( Quang and Donald, 2006).

Isomorphous substitution within the layers (for example,  $\text{Al}^{3+}$  replaced by  $\text{Mg}^{2+}$  or  $\text{Fe}^{2+}$ , or  $\text{Mg}^{2+}$  replaced by  $\text{Li}^{1+}$ ) generates negative charges that are counterbalanced by alkali and alkaline earth cations situated inside the galleries. This type of layered silicate is characterized by a moderate surface charge known as the cation exchange capacity (CEC), and generally expressed as mequiv/100 gm. This charge is not locally constant, but varies from layer to layer, and must be considered as an average value over the whole crystal (Manias *et al.*, 2001; Sinha Ray Okamoto., 2003). Thus, in order to have a successful development of clay-based nanocomposites, it is necessary to chemically modify a naturally hydrophilic silicate surface to an organophilic one so that it can be compatible with a chosen polymer matrix. Generally, this can be done through ion-exchange reactions by replacing interlayer cations with quarternary alkyl ammonium or alkylphospho- ion-exchange reactions cations with cationic surfactants such as those mentioned above render the normally hydrophilic silicatesurface organophilic, thus making it more compatible with non polar polymers .These cationic surfactants modify interlayer interactions by lowering the surface energy of their organic component and improvethe wetting characteristics with the polymer. Furthermore, they can provide functional groups .That can react withthe polymerorinitiate polymerization of monomers and there by improve the strength of the interface between the polymer andinorganic component ( Quang and Donald, 2006).

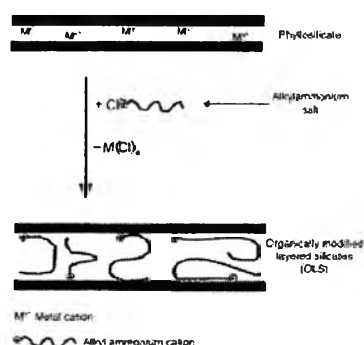


**Figure 2.2** Schematic representation of a cation-exchange reaction between the silicate and an alkyl ammonium salt (Quang and Donald, 2006).

## 2.2 Porous Clay Heterostructure (PCH)

A variety of ordered mesoporous materials have been synthesized by surfactant-templated methods. Porous clay heterostructure (PCH) is a recent class of solid porous materials formed by the intercalation of surfactant within the intragalleries of clays. Various types of expandable clay could be employed such as hectorite, vermiculite, synthetic saponite and montmorillonite for the synthesized of these highly porous clays.

Polverejan *et al.*, (2002) prepared the post synthesis grafting of aluminum into the meso structured intra gallery silica framework of a PCH precursor derived adsorption, from asynthetic saponite clay. Elemental analyses, powder X-ray diffraction , N<sub>2</sub> adsorption and <sup>27</sup>Al MAS NMR spectroscopy were used to characterize the reaction products, which designated Al-SAP/PCH . Depending on the choice of aluminum reagent (AlCl<sub>3</sub> or NaAlO<sub>2</sub> ) ,the Al-SAP/PCH derivatives exhibited basal spacings of 32-34.8 Å, BET surface areas of 623-906 m<sup>2</sup>/g, pore volumes of 0.32-0.45 cm<sup>3</sup>/g, and pore sizes in the large micropore to small mesopore range(14-25 Å).

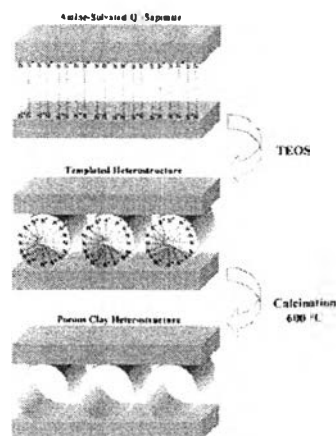


**Figure 2.3** Schematic representation of porous clay hetero structure (PCH) formation. (Polverejan *et al.*, 2002).

Polverejan *et al.* (2000) prepared porous clay heterostructures within the galleries of synthetic saponite clays with targeted layer charge densities in the range  $x = 1.2-1.7 e^-$  units per  $Q^+_x[Mg_6](Si_{8-x}Al_x)O_{20}(OH)_4$  unit cell. The CEC value increase is proportional to the aluminum content of the clays. All three saponites were used to assemble porous clay heterostructures that were denoted SAP1.2-, SAP1.5-, and SAP1.7-PCH, respectively. The removal of the intragallery mixture of neutral alkylamine and quaternary ammonium ion surfactant (Q+) by calcination afforded PCH intercalates with basal spacings of 33-35 Å. The BET specific surface areas progressively decreased with increasing aluminum loading from 921 to 797  $m^2 g^{-1}$  and the framework pore volumes decreased from 0.44 to 0.37  $cm^3 g^{-1}$ . Moreover, these materials exhibited the framework pore sizes were in the supermicropore to small mesopore region 15-23 Å as can be seen in TEM image (Figure 2.4.). In 2000, they synthesized acid-functionalized porous clay heterostructure from synthetic saponite through postsynthesis grafting reactions using  $AlCl_3$  and  $NaAlO_2$  as alumination agents under acid and basic condition, respectively. The amount of tetrahedral aluminum incorporated into the saponite gallery structure is correlated with the concentration of aluminum in the grafting solution. However, some loss of gallery mesostructure occurred at higher aluminum loadings (e.g., Si/Al = 5) with sodium aluminate. Depending on the choice of aluminum reagent ( $AlCl_3$  or  $NaAlO_2$ ), the Al-SAP/PCH derivatives exhibited basal spacings of 32-34.8 Å, BET surface areas of 623-906  $m^2/g$ , pore volumes of 0.32-0.45  $cm^3/g$ , and pore sizes in the large micropore to small mesopore range (14-25 Å).

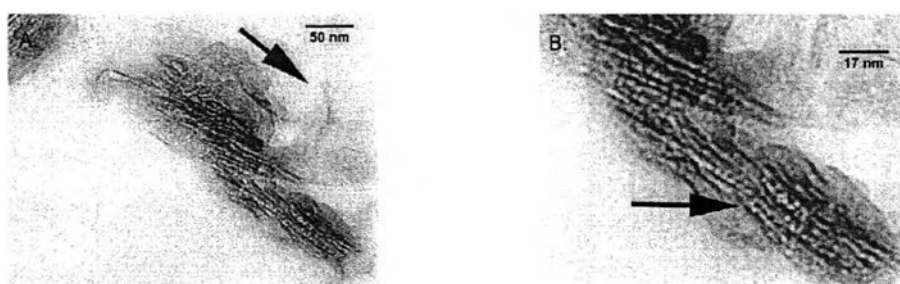


**Figure 2.4** TEM images of saponite heterostructure (Polverejan *et al.*, 2000).

Benjelloun *et al.* (2001) studied the cationic exchange capacities (CECs) of two porous clay heterostructures (PCHs), derived from natural montmorillonite (PMH) and synthetic saponite (PSH). Three methods for the formation of  $\text{NH}_4^+$ -exchanged PCH forms are describe and evaluated: (1) adsorption of ammonia under a gas flow on calcined and extracted PCHs in acidified methanol; (2) direct exchange in  $\text{NH}_4\text{Cl}$  solutions; (3) solvent extraction with  $\text{NH}_4\text{Ac}/\text{EtOH}/\text{H}_2\text{O}$ . The obtained ammonium containing materials are subsequently exchanged for  $\text{K}^+$  cations in aqueous solution in order to determine the CEC of the PCH solids. Several extraction media were tested for their efficiency in extracting the hexadecyltrimethylammonium surfactant from the PCH precursor. The best results were obtained with methanol:water mixture with 9:1 vol%. The resulting extracted materials had a higher specific surface area and porosity and even a slightly narrower pore size distribution than the calcined ones with maxima of  $997 \text{ m}^2/\text{g}$ . and  $0.76 \text{ cm}^3/\text{g}$  for montmorillonite PCH (PMH) and  $1118 \text{ m}^2/\text{g}$  and  $0.97 \text{ cm}^3/\text{g}$  for saponite PCH (PSH).

In 2001, Pichowicz and Mokaya prepared Porous clay heterostructures (PCHs) from suitably acid-activated montmorillonite clays; the higher acidity arises from Bronsted acid sites generated by acid treatment of the clay prior to its use as a host for PCH formation. The results of PCHs and PAACHs (porous acid activated clay heterostructures) are the PCH samples have surface area of  $800 \text{ m}^2/\text{g}$  while the acid-activated clay derived samples have higher surface area of  $915 \text{ m}^2/\text{g}$  for PAACH which is derived from acid activated clay using octylamine and  $951 \text{ m}^2/\text{g}$  for PAACH which is derived from acid activated clay using decylamine . The surface areas of the present materials are generally higher than that of fluorohectorite-PCH but comparable to those of saponite and montmorillonite derived PCHs.

### 2.3 Polylactide or Polylactic Acid ( PLA )

Rhim *et al.*(2008) observed the growth of environmental concerns over non-biodegradable petrochemical based plastic packaging materials has raised interest in

the use of biodegradable alternatives originating from renewable sources (Petersen *et al.*, 1999; Weber *et al.*, 2002). Among the renewable source-based biodegradable plastics, polylactides or poly(lactic acid) (PLA) is one of the most promising materials since it is thermoplastic, biodegradable, biocompatible and has high-strength, high-modulus and good processability (Drumright *et al.*, 2000; Garlotta, 2001). PLA is a linear aliphatic thermoplastic which can either be synthesized by condensation of lactic acid or ring opening polymerization of lactide which is the diester of lactic acid. Lactic acid is a chiral organic acid which mainly occur in the L-form. It is produced by fermentation of dextrose which it self is gained from annually renewable resources like corn ( Bax and Mussig, 2008).

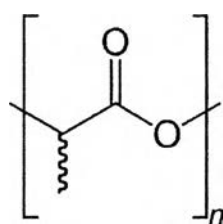


**Figure 2.5** The skeletal formula of polylactic acid (www.wikipedia.com).

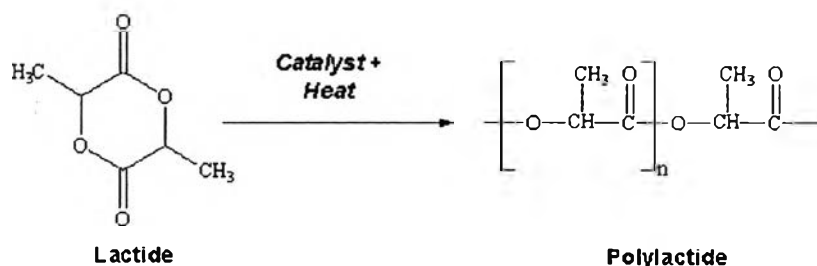


**Figure 2.6.** Synthesis of PLA (www.wikipedia.com).

Due to high production costs, in the early stages of its development PLA was used in limited areas, such as preparation of medical devices (bone surgery, suture, and chemotherapy, etc.). Since production cost has been lowered by new technologies and large-scale production, the application of PLA has been extended to other

commodity areas such as packaging, textiles and composite materials (Drumright, Gruber and Henton, 2000; Garlotta, 2001).

Kikkawa *et al.* (2004) studied effect of water on the surface molecular mobility of Poly ( lactide ) thin films with 300 nm thickness by an atomic force microscopy. Two types of PLAs were applied for the experimental samples as uncrystallizable PLA (uc-PLA) and crystallizable PLA (c-PLA). The amorphous region around the hexagonal crystal in a partially crystallized c-PLA thin film was completely degraded at 20°C within 15 min, whereas the crystalline region remained unchanged in the presence of proteinase K. Thus, the amorphous region around the crystal was preferentially degraded by the enzyme at a fast rate. The surface glass-transition temperature of the amorphous uc-PLA (PLDLA) thin film was determined from the friction and temperature curves. The glass-transition temperature (58°C) for uc-PLA in water was lower than that (70°C) in vacuum conditions, suggesting that water molecules function as a plasticizer and enhance the molecular mobility of PLA molecules on the surface of PLAs. Friction force measurement was also performed on the surface of the amorphous c-PLA(PLLA) thin film as a function of temperature. In addition, the morphological change of c-PLA during heating process was observed by AFM. A cold crystallization temperature for c-PLA was decreased in the presence of water compared with that under vacuum conditions.

## 2.4 Polymer-Clay Nanocomposites

Polymer-clay nanocomposites exhibit outstanding properties that are synergistically derived from the organic and inorganic components. They exhibit superior mechanical properties, reduced gas permeability, improved solvent resistance and enhance ionic conductivity (Galgali *et al.*, 2001).

Polymer-clay hybrid nanocomposites is provided with emphasis placed on the use of alkyl ammonium exchanged smectite clays as the reinforcement phase in selected polymer matrices. A few weight percent loading of organoclay in nylon6 boosts the heat distortion temperature by 808°C, making possible structural applications under conditions where the pristine polymer would normally fail. A

similar loading of clay nanolayers in elastomeric epoxy and polyurethane matrices dramatically improves both the toughness and the tensile properties of these thermoset systems. Glassy epoxy nanocomposites exhibit substantial improvement in yield strength and modulus under compressive stress strain conditions. The latest development in polypropylene hybrids have yielded nanocomposites with improved storage moduli. Polyimide hybrids in thin-film form display a 10-fold decrease in permeability toward water vapor at 2 wt% clay loading. In situ and melt intercalation processing methods are effective in producing reinforced polystyrene hybrids. Nitrile rubber hybrids show improved storage moduli and reduced permeabilitys even toward gases as small as hydrogen. Clay nanolayers dispersed in liquid crystals act as structure direct or sand form hybrids composites that can be switched from being highly opaque to highly transparent by applying an electric field of short duration ( LeBaron *et al.*, 1999 ).

Nanocomposite structures depending on the nature of the components used (layered silicate, organic cation and polymer matrix) and the method of preparation, three main types of composites may be obtained when a layered clay is associated with a polymer (Figure 2.7). When the polymer is unable to intercalate between the silicate sheets, a phase separated composite (Figure 2.7a) is obtained, whose properties stay in the same range as traditional microcomposites. Beyond this classical family of composites, two types of nanocomposites can be recovered. Intercalated structure (Figure 2.7b) in which a single (and sometimes more than one) extended polymer chain is intercalated between the silicate layers resulting in a well ordered multilayer morphology built up with alternating polymeric and inorganic layers. When the silicate layers are completely and uniformly dispersed in a continuous polymer matrix, an exfoliated or delaminated structure is obtained (Figure 2.7c) (Alexandre and Dubois., 2000).



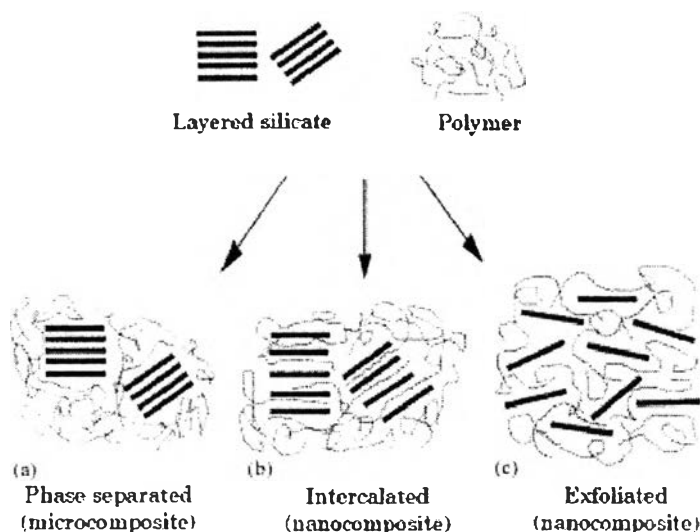


**Figure 2.7** Scheme of different types of composite arising from the interaction of layered silicates and polymers : (a) phase-separated microcomposite; (b) intercalated nanocomposite and (c) exfoliated nanocomposite (Alexandre and Dubois., 2000).

Many researches efforts focus on the preparation of polypropylene-clay nanocomposites. But PP does not include polar groups in its backbone, it was thought that the homogeneous dispersion of the silicate layers in PP would not be realized. Hence, it is frequently necessary to use a compatibilizer such as maleic anhydride modified polypropylene (PP-g-MA). There are two important factors to achieve the exfoliation of the clay layer silicates: (1) the compatibilizer should be miscible with the polypropylene matrix, and (2) it should include a certain amount of polar functional groups in a molecule. Generally, the polypropylenes modified with maleic anhydride (MA) fulfill the two requirements and are frequently used as compatibilizer for polypropylene nanocomposites. However, they have mechanical properties lower than the native polypropylene, due to chain scission during grafting (Lertwimolnum and Vergnes., 2005).

In this work , the nanocomposites is polylactide-clay nanocomposites which mixed by twin screw extruder . In the preparation of polymer/clay nanocomposites, organoclay plays an important role in lipophilizing and dispersing the clay into less

polar polymer matrixes. Organic modifiers of various chain lengths were examined in different types of clays, smectite, montmorillonite (MMT), and mica, to prepare their corresponding organoclays. The layered structure and gallery spacing of organoclays and polylactide (PLA) nanocomposites shows that, with a modifier of the same chain length, the gallery spacing of the organoclay was largest for mica and smallest for smectite because of the higher ion-exchange capacity of mica and physical jamming of the modifier due to a restricted conformation at the core part of the clay of larger size. The increment of the modulus in a smectite nanocomposite, compared to that of PLA, is higher than MMT or mica nanocomposite due to better dispersion in a smectite system for the same clay loading. Being a well-dispersed system, smectite nanocomposites have better gas barrier properties than the MMT or mica systems, which are larger in size but stacked in nature in their nanocomposites. A new idea for obtaining porous ceramic material from layered silicate/polymer nanocomposites by burning is unveiled using various clays and the mechanism of their formation is elucidated (Maiti et al., 2002).

Many research studied in the preparation of polylactide-clay nanocomposite such as Sinha Ray *et al.* (2002) described the preparation, characterization, material properties, and biodegradability of polylactide (PLA)-layered silicate nanocomposite. Montmorillonite modified with trimethyl octadecylammonium cation was used as an organically modified layered silicate (OMLS) for the nanocomposite preparation. WAXD and TEM analyses respectively confirmed that silicate layers of the montmorillonite were intercalated and nicely distributed in the PLA-matrix. The material properties of neat PLA improved remarkably after nanocomposite preparation. The biodegradability of the neat PLA and corresponding nanocomposite was studied under compost, and the rate of biodegradation of neat PLA increased significantly after nanocomposite preparation. In 2002, M. Pluta *et al.* described PLA-clay nanocomposites loaded with 3 wt% organomodified montmorillonite and PLA-clay microcomposites containing 3 wt % sodium montmorillonite were prepared by melt blending and investigated the morphology and thermal properties of the nanocomposites and microcomposites and compared them with unfilled PLA, keeping the same thermomechanical history. The influence of the processing temperature on

the structural characteristics of the investigated systems was determined. The investigations were performed with differential scanning calorimetry (DSC), thermogravimetric analysis (TGA), X-ray diffraction (XRD), size exclusion chromatography (SEC), and polarized light microscopy (LM). XRD showed that the good affinity between the organomodified clay and the PLA was sufficient to form intercalated structure in the nanocomposite. The microcomposite featured a phase-separated constitution. DSC and LM studies showed that the nature of the filler affected the ordering of the PLA matrix at the molecular and supermolecular levels. According to TGA, the PLA-based nanocomposites exhibited improvement in their thermal stability in air. Reduced flammability, together with char formation, was also observed for nanocomposites, compared to the microcomposites and pure PLA.

Solarski *et al.*(2007) studied thermal, mechanical, shrinkage and fire properties of (Plasticized) polylactide-clay nanocomposite textile. This experiment has various quantities of Cloisite<sup>®</sup> 30B (from 1% to 4% in weight) which is the additive used for the preparation of the PLA nanocomposites. The surfactant of the C30B is a methyl tallow alkyl bis-2-hydroxyethyl quaternary ammonium cation. C30B is delivered in the shape of a fine powder have been added to a polylactide matrix by melt blending to produce polylactide-based nanocomposites. The interactions between the carbonyl functions of PLA chains and hydroxyl functions of the alkyl ammonium surfactants surface-covering MMT nanoplatelets seem to improve the dispersion of this organo-clay in a PLA matrix, contrary to other kinds of MMT without hydroxyl functions on the surfactant. Then, these blends have been melt-spun to produce multifilaments yarns. It is demonstrated that it is necessary to use a plasticizer to spin a blend with 4% in weight of Cloisite<sup>®</sup> 30B. The properties of these yarns have been studied (dispersion of the clay, thermal, mechanical and shrinkage properties). A decrease of the tensile properties is observed when the quantity of Cloisite<sup>®</sup> 30B increases, but an improvement of the thermal and shrinkage properties is highlighted. These multifilaments have been knitted and the flammability studied using cone calorimeter at 35 kW/m<sup>2</sup>. A strong decrease, up to 38%, of the heat release rate has been measured.

Gu *et al.* (2007) studied about the linear and nonlinear shear rheological behaviors of polylactide (PLA)-clay (organophilic-montmorillonite) nanocomposites (PLACNs) were investigated by an Advanced Rheology Expanded System rheometer. The nanocomposites were prepared by master batch method using a twin-screw extruder with poly( $\epsilon$ -caprolactone) (PCL) as a compatibilizer. The presence of org-MMT leads to obvious pseudo-solid-like behaviors of nanocomposite melts. The behaviors caused by the formation of a “percolating network” derived from the reciprocity among the strong related sheet particles. Therefore, the storage moduli, loss moduli, and dynamic viscosities of PLACNs show a monotonic increase with MMT content. Nonterminal behaviors exists in PLACNs nanocomposites. Besides the PLACNs melts show a greater shear thinning tendency than pure PLA melt because of the preferential orientation of the MMT layers. Therefore, PLACNs have higher moduli but better processibility compared with pure PLA .

## 2.5 Applications of Mesoporous Clay in Entrapping Systems

The first major challenge for the adsorption field is to select the most promising types of sorbent form and extremely large readily available materials. The usage of natural mineral adsorbents is increasing because of their abundance and low price. Due to the ability to form mesoporous materials with closely reproducible pore size of the PCH and the ability to control surface properties of the hybrid organic-inorganic PCH, adsorption properties of these materials obtained from the intercalation of clays attracted the interest. The most extensive work dealt with the adsorption of heavy metals.

Mercier and Pinnavaia (1998) demonstrated the first potential environmental application of a porous clay heterostructure. A heavy metal ion adsorbent that bind  $\text{Hg}^{2+}$  ions was prepared by grafting 3-mercaptopropyltrimethoxysilane to the intragallery framework walls of a porous fluorohectorite clay heterostructure (PCH) as illustrated in Figure 2.8. The results revealed that the immobilized thiol groups (up to 67%) were accessible for  $\text{Hg}^{2+}$  trapping.

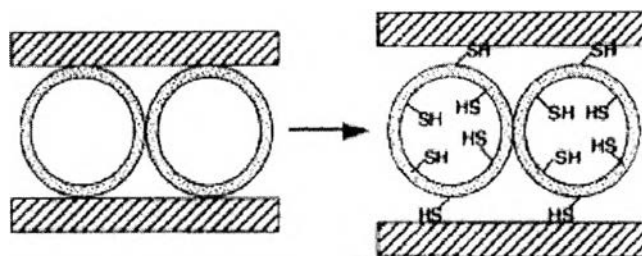


**Figure 2.8** Grafting of mercaptopropylsilane groups to the inner and outer walls of mesostructural silica intercalated in smectite clay (Mercier and Pinnavaia, 1998).

The adsorption properties of PCH have been considered in a number of studies, particularly when considering adsorption process as the recovery of volatile organic compounds or the enrichment of the more valuable fractions of natural or land fill gas. In 2004, Pires *et al.* prepared porous materials from a natural smectite by the gallery templated approach, using a quaternary ammonium cation (CTAB) and neutral amines with different chain length (octylamine and decylamine). The materials prepared in this work, after calcination at 650°C, had  $A_{BET}$  values in the range of 600–700  $m^2 g^{-1}$  and micropore volumes near 0.3  $cm^3 g^{-1}$ . Furthermore, the samples presented pores with widths in the transition between micro to mesopores. The possibility of using such materials as adsorbents of volatile organic compounds, due to their textural and hydrophobic characteristics, was studied by the adsorption of ethanol and methyl ethyl ketone and water for comparison. The data from the adsorption showed that particularly one sample where decylamine was used in the synthesis, has interesting properties regarding the adsorption of VOCs.

## 2.6 Magnetic Properties

Magnetic materials are one of the most prominent classes of functional materials. They are mostly inorganic, metallic or ceramic in nature and typically multi component when used in applications such as alloys or intermetallic phases. Their structure can be amorphous or crystalline with grain sizes ranging from a few nanometers (as in high-end nanocrystalline soft magnetic materials) to centimeters (as

in grain-oriented transformer steels). They are available as powders, cast, sintered or composite materials, ribbons or even thin films and find a huge variety of applications in transformers, motors, generators, medical system sensors, and microelectronic devices. Empirically, materials are classified according to their response to an applied magnetic field, i.e. the magnetization induced by the external field. A more fundamental understanding results from considering the microscopic mechanisms that determine the behavior of materials in the magnetic field. The types of magnetic are diamagnetism, paramagnetism and ferromagnetism.

1. Diamagnetism is a property of all materials. It results from an additional orbital angular momentum of electrons induced in a magnetic field. In analogy to the induction of eddy currents in a conductor it manifests itself as a magnetization oriented in the opposite direction to the external field.

2. Paramagnetism means a positive magnetic susceptibility, i.e. the induced magnetization is along the direction of the external magnetic field. It is observed in materials which contain atoms with nonzero angular momentum, e.g. transition metals. The susceptibility scales with  $1/T$  ( Curie is law). Paramagnetism is also found in certain metals as a consequence of the spin of conduction electrons. The related susceptibility is essentially independent of temperature. The paramagnetic susceptibility is generally several orders of magnitude larger than the diamagnetic component; therefore, diamagnetism is not observable in the presence of paramagnetism.

3. Ferromagnetism describes the fact that certain solid materials exhibit a spontaneous magnetization,  $M_s$ , even in the absence of an external magnetic field. It is a collective phenomenon resulting from the spontaneous ordering of the atomic magnetic moments due to the exchange interaction among the electron spins. It is observed in a few transition metals where itinerant electrons play the essential role for the exchange coupling mechanism, but also in their oxides, halides etc., where the exchange interaction is mediated by localized electrons of oxygen, sulfur etc. atoms located between neighboring metal atoms (indirect exchange, superexchange). Many ferromagnetic objects do not show a net magnetization without an external magnetic field. This is a consequence of magnetic domains, which are formed to reduce the

energy connected with the dipolar fields. When an external magnetic field is applied domains gradually vanish due to the motion of domain walls and rotation of the magnetization inside the domains. These processes are partly reversible and irreversible. In sufficiently high fields technical saturation is achieved. The corresponding saturation magnetization, however, must not be mistaken for the spontaneous magnetization. The reason is that, at any temperature  $T > 0$ , an external field will increase the magnetization above the spontaneous value inside the domains by suppression of spin waves (the para-process). Hence, the experimental determination of the spontaneous magnetization in general requires a specific extrapolation of high field data to zero field (Harada *et al.*)

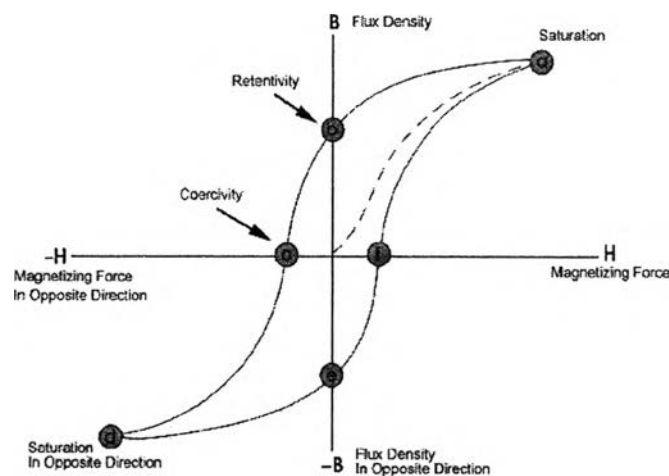


**Figure 2.9** Schematic representation of a hysteresis loop for a ferromagnetic material in an magnetic field ([www.ndt-ed.org](http://www.ndt-ed.org)).

Many researches efforts focus on the preparation of the magnetite particles. Ferric chloride hexahydrate and ferrous chloride tetrahydrate are used as iron sources, and aqueous ammonia is used as the precipitator. Distilled water is used as the solvent. The corresponding phase  $\text{NH}_4\text{OH}$  was slowly injected into the mixture of  $\text{FeCl}_3$  and  $\text{FeCl}_2$  under vigorous stirring. After precipitation, the  $\text{Fe}_3\text{O}_4$  particles were repeatedly washed and filtered before drying at room temperature in air atmosphere to

form powders. Before the reaction, N<sub>2</sub> gas was flown through the reaction medium to prevent possible oxidation. The reaction was operated in a closed system to provide a nonoxidation environment. Otherwise, Fe<sub>3</sub>O<sub>4</sub> might also be oxidized which means the suspension will turn from black to yellow and will affect the purity of the final production. The Fe<sub>3</sub>O<sub>4</sub> nanoparticles prepared by co-precipitation were dried at room temperature in air atmosphere to form a powder, which they called the powder sample. Fe<sub>3</sub>O<sub>4</sub> powder was put into 6 ml distilled water to form the aqueous solution and then HCl added to the aqueous solution to a pH of 2. After ultrasonic shocking of the aqueous solution, the Fe<sub>3</sub>O<sub>4</sub> nanoparticles were well dispersed in the distilled water and then the solution formed, which they called the dispersed suspension sample. The structural properties of Fe<sub>3</sub>O<sub>4</sub> nanoparticle powders were analyzed by X-ray diffraction, the mean size and morphologies of Fe<sub>3</sub>O<sub>4</sub> particles were observed by transmission electron microscopy and a vibrating sample magnetization was used to evaluate the magnetic parameters (Liu *et al.*, 2002).